BIOCHEMISTRY
including biophysical chemistry & molecular biology

Article

pubs.acs.org/biochemistry

Competition Between Homodimerization and Cholesterol Binding to the C99 Domain of the Amyloid Precursor Protein

Yuanli Song,[†] Eric J. Hustedt,[‡] Suzanne Brandon,[‡] and Charles R. Sanders*[,†]

[†]Department of Biochemistry and Center for Structural Biology, Vanderbilt University School of Medicine, Nashville, Tennessee 37232, United States

[‡]Department of Molecular Physiology and Biophysics, Vanderbilt University School of Medicine, Nashville, Tennessee 37232, United States

Supporting Information

ABSTRACT: The 99-residue transmembrane C-terminal domain (C99, also known as β-CTF) of the amyloid precursor protein (APP) is the product of the β-secretase cleavage of the full-length APP and is the substrate for γ-secretase cleavage. The latter cleavage releases the amyloid-β polypeptides that are closely associated with Alzheimer's disease. C99 is thought to form homodimers; however, the free energy in favor of dimerization has not previously been quantitated. It was also recently documented that cholesterol forms a 1:1 complex with monomeric C99 in bicelles. Here, the affinities for both homodimerization and cholesterol binding to C99 were measured in bilayered lipid vesicles using both electron paramagnetic resonance (EPR) and Förster resonance energy transfer (FRET) methods. Homodimerization and cholesterol binding were seen to be competitive processes that center on the transmembrane $G_{700}XXXG_{704}XXXG_{708}$ glycine-zipper motif and adjacent Gly709. On one hand, the observed K_d for cholesterol binding (K_d = 2.7 ± 0.3 mol %) is on the low end of the physiological cholesterol concentration range in mammalian cell membranes. On the other hand, the observed K_d for homodimerization (K_d = 0.47 ± 0.15 mol %) likely exceeds the physiological concentration range for C99. These results suggest that the 1:1 cholesterol/C99 complex will be more highly populated than C99 homodimers under most physiological conditions. These observations are of relevance for understanding the γ-secretase cleavage of C99.

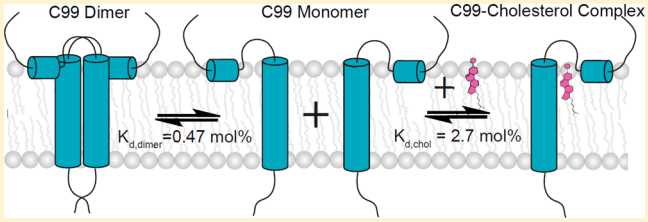

It is generally believed that the etiology of Alzheimer's disease (AD) is closely related to the production of the amyloid-β (Aβ) polypeptides, with factors that result in higher overall Aβ concentrations or that favor an increased production of the long forms of Aβ relative to the short forms being regarded as pro-AD factors.[1−4] Accordingly, there is great interest in elucidating the molecular mechanisms of amyloidogenesis. This study focuses on the biochemical and biophysical properties of a key protein intermediate in the amyloidogenic pathway, C99 (Figure 1). C99 is the transmembrane 99 residue C-terminal domain of the amyloid precursor protein (APP) that is generated upon the cleavage of APP by β-secretase. C99 is also the immediate precursor of the Aβ polypeptides, which are released when C99 is cleaved by γ-secretase. The mechanisms responsible for the regulation of substrate recognition and the subsequent cleavage of C99 by γ-secretase are not well understood. However, there is considerable evidence that elevated cholesterol levels enhance the amyloidogenic pathway of APP processing and inhibit a competing nonamyloidogenic cleavage pathway.[5−14] These observations may be related to the recent discovery that C99 (and possibly full-length APP) is a cholesterol-binding protein.[15]

Much attention has also been paid to the possible homodimerization of C99 and its impact on cleavage of C99 by γ-secretase. The transmembrane domain (TMD) of C99 contains both a glycine-zipper sequence ($G_{700}XXXG_{704}XXXG_{708}$) and an adjacent $G_{709}XXXA_{713}$ motif. These common motifs sometime contribute to the homo- or heterodimerization of membrane proteins by promoting intimate and adhesive helix-to-helix contacts.[16−19] There is now considerable evidence that C99 can form homodimers,[20−35] with most data pointing to the surface provided by the Gly sites of the $G_{700}XXXG_{704}XXXG_{708}$ zipper as the central interface.[20,26,28,29,31,35] This notion has prompted studies in which the effect of Gly mutations on γ-secretase cleavage in model mammalian cell lines has been tested.[26−29] The results of these studies were originally interpreted mainly in terms of the potential impact of alterations in homodimerization on γ-secretase cleavage, but they may now need to be revisited in light of data that suggests that these same sites are involved in cholesterol binding.[15]

The actual avidity of homodimerization (as reflected by K_d) has not been rigorously quantitated. Moreover, the fact that both dimerization and cholesterol binding seem to involve the same glycine-zipper motif in the transmembrane domain raises questions about the possible relationship of cholesterol binding to homodimerization and γ-secretase cleavage. Most impor-

Received: June 10, 2013
Revised: June 29, 2013
Published: July 6, 2013

   dx.doi.org/10.1021/bi400735x | *Biochemistry* 2013, 52, 5051−5064

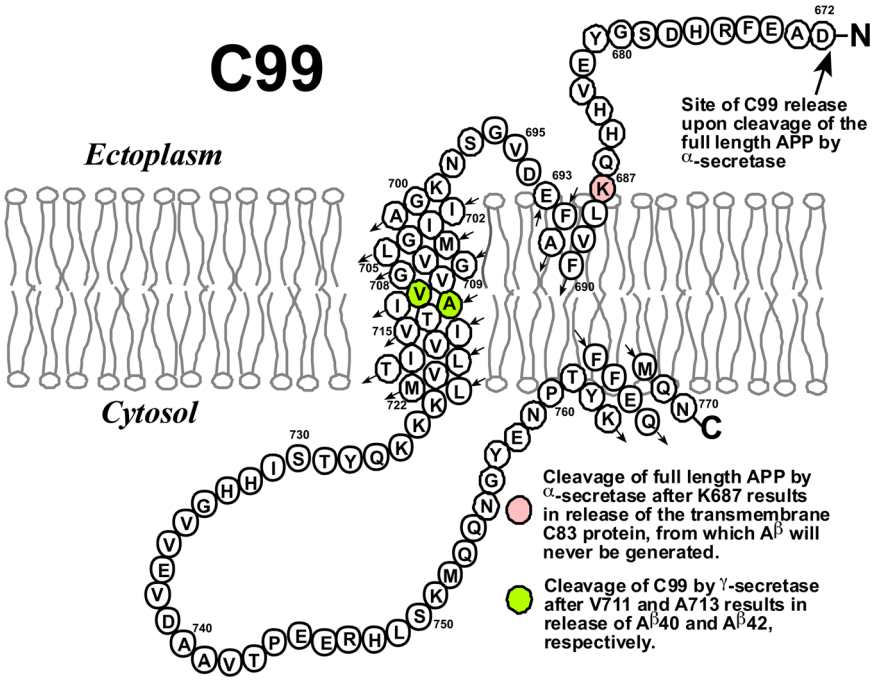

Figure 1. Topology map of the C99 protein. Not depicted is the hinge-like kink located in the transmembrane helix that occurs at $G_{708}G_{709}$.[15]

tantly, are these competitive processes? Given that the cholesterol concentration present in the plasma membranes of mammalian cells is well above the 5 mol % K_d measured for 1:1 complex formation with C99 in bicelles,[15,36] an understanding of the relationship between homodimerization and cholesterol binding is needed to illuminate the final biochemical step of the amyloidogenic pathway in living cells.

Here, we quantitate the homodimerization of C99 in bilayered lipid vesicles and show that self-association is of only modest avidity. We also measure the K_d for cholesterol binding under the same conditions and demonstrate that cholesterol binding to the C99 monomer and protein homodimerization are competitive processes, with both involving the $G_{700}XXXG_{704}XXXG_{708}$ zipper motif.

METHODS

Chemicals. Sodium dodecylsulfate (SDS), lyso-myristoylphosphatidylglycerol (LMPG), 1-palmitoyl-2-oleoylphosphatidylcholine (POPC), and 1-palmitoyl-2-oleoyl-phosophatidylglycerol (POPG) were purchased from Anatrace-Affymetrix (Maumee, OH) and Avanti (Alabaster, AL). Thiol-activated spin label, 1-oxyl-2,2,5,5-tetramethylpyrroline-3-methyl-methanethiosulfonate (MTSL), was purchased from Toronto Research Chemicals (Toronto, ON). Fluorescent labels *N*,*N*-dimethyl-*N*-(iodoacetyl)-*N*-(7-nitrobenz-2-oxa-1,3-diazol-4-yl)-ethylenediamine (IANBD) and 5-((((2-iodoacetyl)amino)-ethyl)amino)naphthalene-1-sulfonic acid (IAEDANS) were purchased from Invitrogen (Carlsbad, CA). All other chemicals were from Sigma (St. Louis, MO).

Expression, Purification, and Spin Labeling of Wild-Type and Mutant Forms of C99. As described previously,[15,20] human C99 was expressed in *E. coli* and purified using metal-ion affinity chromatography into micelles composed of either 0.05% LMPG or 0.2% SDS.

Wild-type C99 has no Cys residues. Selected residues were mutated to cysteine using the QuikChange method utilizing whole-plasmid PCR (Stratagene, CA, USA). A total of 11 single Cys C99 mutants were prepared: S697C, G700C, A701C, I702C, I703C, G704C, L705C, G708C, G709C, A713C, and S730C.

The single Cys C99 mutants were spin labeled as previously described,[15] resulting in final solutions containing pure spin-labeled C99 in a buffer containing 0.2% SDS and 250 mM imidazole, pH 7.8. The spin-labeling efficiency for each C99 sample was quantitated by double-integrating EPR resonances from each labeled sample relative to the signal from a 100 μM TEMPOL standard. The estimated spin-label concentration was then compared to the protein concentration determined by UV absorbance at 280 nm using an extinction coefficient of 5960 M^{-1} cm^{-1}. In all cases, the spin-labeling efficiency was >90%.

Fluorescent Labeling of Single Cys C99 Mutants. The S730C C99 mutant was purified into 0.05% LMPG and treated with DTT to ensure the complete reduction of the cysteines, as described previously.[15] This mutant was previously employed in FRET studies of C99 dimerization in detergent micelles using an approach similar to the one used here.[35] For FRET experiments, separate batches of S703C C99 were labeled with thiol-reactive probes IANBD (as an acceptor) and IAEDANS (as a donor). The protein solution was first desalted using a PD-10 column (GE Healthcare, NJ) and equilibrated in a solution of 20 mM Tris-HCl and 150 mM NaCl, pH 7.8 containing 0.05% LMPG. Labeling was then initiated by the immediate addition of a 10× molar excess of IANBD (from a 2 mM stock in acetonitrile) to the protein solution. The resulting mixture was incubated at room temperature in the dark for 1 h and then loaded onto a PD-10 size-exclusion column equilibrated and eluted with a solution of 20 mM Tris-HCl and 150 mM NaCl, pH 7.8 containing 0.2% SDS. The labeling of S730C with IAEDANS was performed in an analogous manner. The degree of labeling was calculated on the basis of the concentration of the protein (determined from A_{280}) and the concentration of IANBD (determined from A_{472} with ε_{472} =

23 700 M^{-1} cm^{-1}) or IAEDANS (determined from A_{337} with ε_{337} = 5600 M^{-1} cm^{-1}).

Reconstitution of C99 into Lipid Vesicles. The reconstitution of C99 into pH 6.5 lipid vesicles was initiated using spin- or fluorescently labeled C99 prepared as described above in a Tris-HCl buffer containing 0.2% SDS. Labeled C99 in 0.2% SDS was concentrated using an Amicon Ultra-15 centrifugal filter (molecular weight cutoff = 10 kDa; Millipore, MA) to a final concentration of 1 mM. The concentrated C99 solution was then mixed with a stock SDS/lipid mixture (400 mM SDS, 75 mM POPC, and 25 mM POPG) with or without cholesterol, resulting in a clear solution that was subjected to >15 freeze/thaw cycles to ensure the complete conversion to mixed micelles. The C99/mixed-micellar mixture was then subjected to extensive dialysis in Spectra/Pro dialysis tubing (molecular weight cutoff = 15 kDa; Spectrum Laboratories, Inc., CA) at room temperature to remove all SDS; this process is accompanied by the formation of C99/POPC/POPG vesicles (with or without cholesterol). To ensure the complete removal of SDS, the 4 L of dialysis buffer (100 mM imidazole and 1 mM EDTA, pH 6.5) was changed twice daily for 5 days. The SDS removal was deemed completed when the C99/lipid solution became cloudy (because of vesicle formation) and the surface tension of the dialysate indicated the complete removal of SDS.

Continuous Wave (CW) EPR Measurements. To assess the dimerization of C99, the C99/lipid mole ratio in 3:1 POPC/POPG lipid vesicles was varied from 1:800 to 1:50. To investigate the effects of cholesterol on dimerization, one experiment was performed in which the C99/lipid mole ratio was varied from 1:800 to 1:50 in vesicles that contained not only the usual 3:1 POPC/POPG but also 20 mol % cholesterol, where mol % cholesterol = 100[moles cholesterol/(moles POPC + moles POPG + moles cholesterol)]. An additional experiment involved fixing the ratio of C99/lipid at 1:100 while cholesterol was varied from 0 to 30 mol %. X-band CW-EPR spectra were collected at 9.81 GHz on a Bruker EMX spectrometer with a TM110 cavity (BrukerBiospin, Billerica, MA) using a 5 mW microwave power source and 1 G field modulation at 100 kHz. The spin-labeled C99 samples were prepared as described above, and 20 μL of each sample was transferred to 50 μL glass capillaries. All EPR spectra were collected at 298 K.

Analysis of the EPR Data. Most of the CW EPR spectra of the spin-labeled C99 mutants exhibited two components characterized by different motional properties. If it is assumed that the narrow component arises from a population of monomer in equilibrium with a population of dimer that yields the broad component, then the dependency of the position of the momoner−dimer population as a function of the protein/lipid ratio can be monitored by measuring the ratio-dependent intensity of any point in the superimposed pair (monomer + dimer) of spectra that is sensitive to the monomer/dimer equilibrium. This approach is similar to that used in previous EPR studies to quantitate binding equilibria.[28,29] We chose to monitor both the intensity of the signal of the field at which the monomer has its highest intensity (3474 G) and the intensity of the field where the dimer component is most evident (3464 G). The dependency of the these intensities as a function of the mole fraction of protein relative to total lipid + protein was fit by a model for homodimerization.

FRET Measurements. To assess the homodimerization of C99, samples were prepared in which donor-IAEDANS-labeled S730C C99 was reconstituted into lipid vesicles at a fixed donor-labeled S730C C99/lipid ratio of 1:800 (mol/mol) with varying amounts of acceptor-IANBD-labeled S730C C99 at donor/acceptor mole ratios of 1:0, 1:1, 1:2, 1:4, 1:6, 1:8, and 1:16. This results in total C99/lipid ratios of 1:800, 1:400, 1:267, 1:160, 1:114, 1:89, and 1:47, respectively. To investigate the effects of cholesterol on dimerization, a mixture of donor- and acceptor-labeled C99 S730C (1:4 donor/acceptor) was reconstituted into vesicles with a constant C99/lipid mole ratio of 1:100 in the presence of varying levels of cholesterol (0, 5, 10, 15, 20, and 30 mol %). Steady-state fluorescence emission spectra were collected at 298 K using a FluoroMax-3 spectrometer from 400 to 600 nm, with the excitation wavelength at 339 nm. For both sets of experiments, the fraction of dimer in each sample was calculated from the decrease in the emission intensity of the donor (at 474 nm) resulting from the energy transfer to the acceptor. The data were fit to the appropriate competitive-binding models using Origin 8.0.

Fitting of the EPR and FRET Titration Data. The fraction of the dimer (f_D) in a C99 monomer−dimer equilibrium can be expressed as a function of the dissociation constant K_d and the total concentration of C99

$$f_D = \frac{2[D]}{[T]} = \frac{2[D]}{2[D] + [M]} = \frac{2[M]}{K_d + 2[M]} \quad (1)$$

where [D] is the concentration of the C99 dimer, [M] is the concentration of the C99 monomer, and [T] is the total C99 concentration of C99 (equal to [M] + 2[D]), with all values given in mol % concentration units. The dissociation constant K_d is given by

$$K_d = \frac{[M]^2}{[D]} \quad (2)$$

where [M] is the concentration of the C99 monomer and [D] = ([T] − [M])/2. Because the assumption cannot be made that [M] = $[C99]_{total}$, [M] in eq 1 must be its analytic value:

$$[M] = \frac{(K_d{}^2 + 8K_d[T])^{1/2} - K_d}{4} \quad (3)$$

Substituting eq 3 for [M] in eq 1 leads to

$$f_D = \frac{(-K_d + (K_d{}^2 + 8K_d[T])^{1/2}}{(K_d + (K_d{}^2 + 8K_d[T])^{1/2}} \quad (4)$$

f_D can also be expressed with experimental FRET data as

$$f_D = \frac{F_D - F_{DA}}{F_D - F_S} \quad (5)$$

where F_{DA} and F_D are the donor intensities at 474 nm in the presence and absence of acceptor-labeled C99, respectively, and F_S is the donor intensity at 474 nm at saturation. However, F_S is not directly observed experimentally. The combination of eqs 4 and 5 gives

$$\frac{F_D - F_{DA}}{F_D - F_S} = \frac{-K_d + (K_d{}^2 + 8K_d[T])^{1/2}}{K_d + (K_d{}^2 + 8K_d[T])^{1/2}} \quad (6)$$

The rearrangement of eq 6 leads to

$$F_{DA} = F_D - \frac{(F_D - F_S)(-K_d + (K_d{}^2 + 8K_d[T])^{1/2}}{K_d + (K_d{}^2 + 8K_d[T])^{1/2}} \quad (7)$$

dx.doi.org/10.1021/bi400735x | Biochemistry 2013, 52, 5051−5064

A similar equation for the EPR intensity as a function of the concentration of C99 is

$$I_X = I_M - \frac{(I_M - I_S)(-K_d + (K_d{}^2 + 8K_d[T])^{1/2}}{K_d + (K_d{}^2 + 8K_d[T])^{1/2}} \quad (8)$$

where I_X is the observed EPR intensity at X Gauss (where X is any field at which the spectrum varies in intensity as a function of f_D), I_M is the intrinsic EPR intensity of the monomer at X Gauss, I_S is the intrinsic EPR intensity at X Gauss at saturation, and I_X is the observed EPR intensity at X Gauss. The K_d values were obtained by fitting eqs 4, 7, or 8 to the appropriate EPR- or FRET-monitored titration data with Origin 8.0.

When cholesterol was titrated into a sample containing 1 mol % C99, cholesterol can bind to the C99 monomer, leading to two competing equilibria

$$D \rightleftarrows M + M \quad (9)$$

which is described by $K_{d,dimer}$, and

$$M + L \rightleftarrows ML \quad (10)$$

which is described by $K_{d,chol}$. The combination of eqs 9 and 10 gives

$$D + 2L \rightleftarrows 2ML \quad (11)$$

where D is the C99 dimer, L is the cholesterol, and ML is the C99−cholesterol complex.

The superequilibrium constant K of reaction 11 can be written as

$$K = \frac{K_{d,dimer}}{(K_{d,chol})^2} = \frac{[ML]^2}{[D][L]^2} \quad (12)$$

where [ML] is the concentration of the C99−cholesterol complex, $K_{d,dimer}$ is the dissociation constant for C99 dimerization, and $K_{d,chol}$ is the dissociation constant for the C99−cholesterol complex. In this case, the total cholesterol ($[L_t] = [L] + [ML]$) was a variable and the total C99, [T], equals 2[D] + [ML], which was experimentally held constant at 1 mol %. f_D is a function of the superequilibrium constant K from eq 12 and the total concentration of cholesterol $[L_t]$ as follows:

$$f_D = 200(-(K([L_t] - 0.01)^2 + 0.04) + ((K([L_t] - 0.01)^2 + 0.04)^2 + 0.0016(K([L_t] - 0.01) - 1)))^{1/2} /8(K([L_t] - 0.01) - 1) \quad (13)$$

For EPR data with cholesterol, we present

$$f_D = \frac{I_X - I_0}{I_s - I_0} \quad (14)$$

where I_X is the observed EPR intensity at X Gauss (where X is any field at which the spectrum varies in intensity as a function of f_D), I_0 is the EPR intensity at X Gauss in the absence of cholesterol, and I_s is the EPR intensity at X Gauss at saturation. The combination of eqs 13 and 14 gives

$$I_X = I_0 + 200(I_S - I_0) (-(K([L_t] - 0.01)^2 + 0.04) + ((K([L_t] - 0.01)^2 + 0.04)^2 + 0.0016(K([L_t] - 0.01) - 1)))^{1/2} /(8(K([L_t] - 0.01) - 1)) \quad (15)$$

For the FRET data in the presence of cholesterol,

$$f_D = \frac{F_{obs} - F_0}{F_s - F_0} \quad (16)$$

where F_{obs} is the observed intensity at any wavelength that varies because of a cholesterol-based alteration in protein-donor/protein-acceptor dimerization, F_0 is the intensity at that same wavelength without cholesterol, and F_s is the intensity at saturation. The combination of eqs 13 and 16 gives

$$F_{obs} = F_0 + 200(F_S - F_0) (-(K([L_t] - 0.01)^2 + 0.04) + ((K([L_t] - 0.01)^2 + 0.04)^2 + 0.0016(K([L_t] - 0.01) - 1)))^{1/2} /(8(K([L_t] - 0.01) - 1)) \quad (17)$$

The K value was obtained by fitting eq 15 (EPR data) or 17 (FRET data) to the data using Origin 8.0. The $K_{d,chol}$ value was then calculated from eq 12 in conjunction with the value of $K_{d,dimer}$ determined independently from the EPR and FRET C99 titrations in the absence of cholesterol.

RESULTS

All studies in this work were conducted using purified C99 that was reconstituted into bilayered liquid crystalline-phase lipid vesicles containing 3:1 (mol/mol) POPC and POPG, with the latter conferring a net anionic charge (as present in biological membranes). This lipid composition is similar to lipid mixtures commonly used in studies of mammalian membrane proteins and the conditions used in our previous EPR studies of the topology and structure of C99.[15] This work employed a series of single-cysteine-mutant forms of C99, which has no wild-type cysteine residues. It was previously shown that the Cys mutations are nondisruptive to the membrane topology and structure of C99.[15]

Use of EPR and FRET Spectroscopy to Quantitate C99 Monomer−Dimer Equilibrium. Single-cysteine-mutant forms of C99 were spin labeled, reconstituted into bilayered vesicles, and subjected to continuous wave (CW) EPR. Spectra were acquired as a function of the C99/lipid mole ratio. Shown in Figure 2 are the spectra for C99 that is spin labeled at a site either in the solvent-exposed loop immediately N-terminal to the TMD (S697C, Figure 2A) or within the transmembrane domain (L705C, Figure 2B). At the lowest C99 concentration (1:800 C99/lipid), the lineshapes for both mutants appear to be dominated by a single narrow component, which is consistent with intermediate motion. As the protein/lipid ratio increases, the lineshapes become more complex as the contribution from a second, broader component grows. This broader component is clearly evident at the low- and high-field wings of the spectrum for samples with higher protein/lipid ratios. On the basis of the preliminary assumption that these

dx.doi.org/10.1021/bi400735x | Biochemistry 2013, 52, 5051−5064

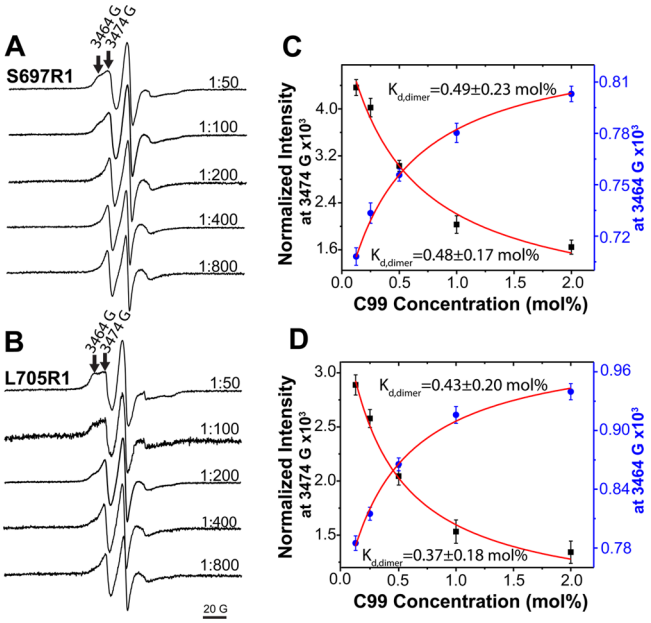

Figure 2. (A, B) CW EPR spectra of spin-labeled C99 in lipid vesicles with different protein/lipid molar ratios (from 1:800 to 1:50). S697R1 (panel A) is the spin-labeled S697C mutant, and L705R1 (panel B) is the spin-labeled L705C mutant. Site 697 is located outside of the TMD, whereas site 705 is located inside the TMD. The arrows in the top trace of each series of spectra indicate the peaks at 3464 (left) and 3474 (right) G. (C, D) EPR intensities at 3474 and 3464 G from panels A and B, respectively, were plotted as a function of the total C99 concentration and fit by a homodimerization model (eq 8).

EPR spectra represent the superimposed resonances from the monomer (narrow component) and dimer (broad component) at equilibrium, we selected two fields in the spectrum that were dominated by the putative monomer and dimer resonances and plotted their changes in intensities as a function of the mol % concentration of spin-labeled C99 in the vesicles (Figure 2C,D). Each data set was then fit to a model (Methods) describing the concentration dependence of the position of the monomer−dimer equilibrium, as shown in Figure 2C,D. A similar approach for using EPR data to quantitate binding-titration data has previously been reported.[37,38] In all cases, the data were well fit by this model regardless of which region of the spectrum was used to extract the intensities. Moreover, approximately the same K_d value for each spin-labeled site was determined regardless of whether the monitored spectral region was dominated by the loss of monomer occurring at higher protein concentrations or by the appearance of dimer. Finally, the K_d values were similar when the measurements were made using data from a spin label either at the water-exposed S697C site or at the membrane-buried L705C site. The average K_d value from these four measurements was 0.44 ± 0.15 mol %. The high degree of self-consistency of the data and the fits are consistent with a monomer−dimer equilibrium. The simplest explanation for the concentration-dependence of the EPR spectra is that C99 populates a mostly monomeric state at a 1:800 protein/lipid ratio and a mostly dimeric state at a 1:50 ratio. There was no evidence for higher-order oligomerization or aggregation, which may have been present in the samples from a previous study[39] that focused on a peptide corresponding to the isolated transmembrane domain of C99 at a significantly higher level of protein (1:30 peptide/lipid) than the highest level examined in this work. The breadth of the EPR signal arising from this putative dimer can be explained as arising from partial immobilization of the Cys-attached spin labels resulting from quaternary structure formation and/or dipolar interaction between the now-proximal pairs of spin labels. The validity of the approach taken to determine K_d from the titration spectra does not depend on the mechanism of line broadening.

Use of FRET to Quantitate Homodimerization. The structural transition detected by EPR is a reversible monomer-to-dimer event that was verified by fluorescence measurements in which FRET was measured as a constant amount of donor-labeled C99 mutant in vesicles was titrated by the same mutant labeled with a FRET acceptor. In this case, the reduction of the signal from the constant donor-labeled C99 present in the FRET data is due to the increasing amount of acceptor-labeled protein. A plot of the data for the loss of donor fluorescence intensity as a function of the total C99 concentration can be fit very well by a by a model for homodimerization, with a derived K_d of 0.51 ± 0.13 mol % that is similar to that determined from the two EPR data sets (Figure 3). The concurrence of the C99/lipid ratio dependence of the EPR and FRET data sets indicates that C99 homodimerizes with a K_d value of 0.47 ± 0.15 mol % (the average of all measured $K_{d,dimer}$ values). We note that a similar approach was previously used to document the homodimerization of C99 in detergent micelles,[35] although the derived K_d value was determined in bulk molarity units, which is not appropriate for the thermodynamic analysis of a molecular association event that occurs between two molecules that are associated with a model membrane phase.[40]

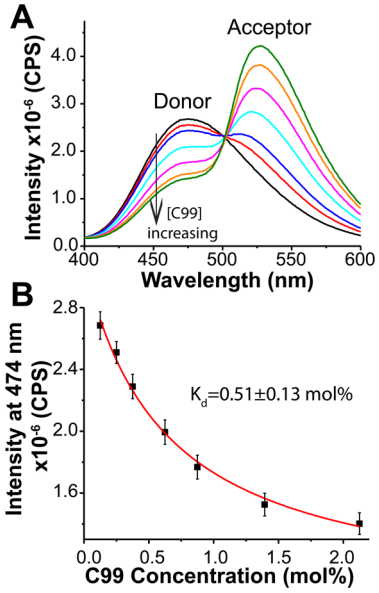

Figure 3. FRET spectra of IAEDANS-labeled C99 S730C (donor) and IANDB-labeled C99 S730 (acceptor) in lipid vesicles. (A) IAEDANS-labeled C99 (donor) was reconstituted into lipid vesicles with a protein/lipid molar ratio of 1:800 (black) with increasing amounts of IANDB-labeled C99 (acceptor). Acceptor IANDB-labeled C99 (acceptor) was increased relative to donor IAEDANS-labeled C99 over the following protein/protein molar ratios: 1:1 (red), 1:2 (blue), 1:4 (cyan), 1:6 (magenta), 1:8 (orange), and 1:16 (green), which correspond to total C99/lipid molar ratios of 1:400, 1:267, 1:160, 1:114, 1:89, and 1:47, respectively. (B) Intensity at 474 nm in each spectrum was plotted as a function of the total C99 concentration and then fit by a model for homodimerization (eq 7).

dx.doi.org/10.1021/bi400735x | Biochemistry 2013, 52, 5051−5064

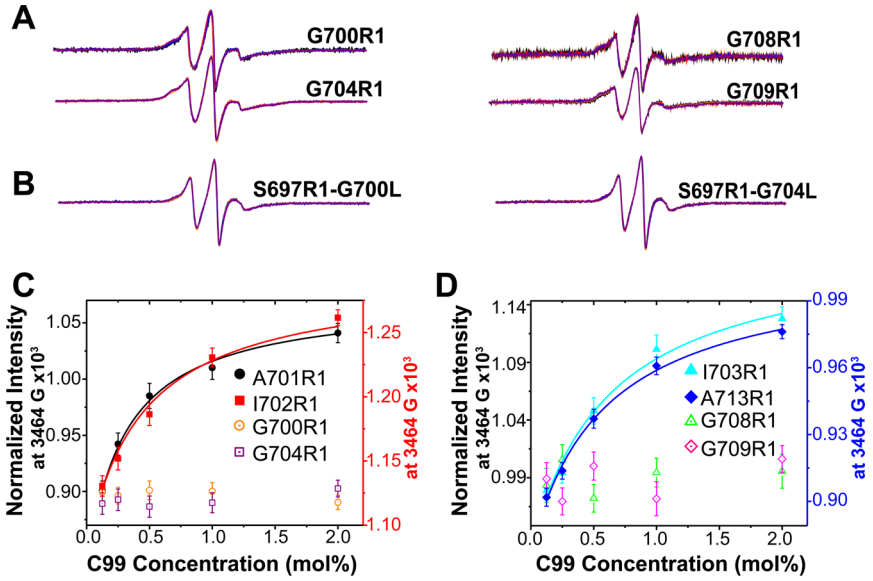

Figure 4. CW EPR spectra of spin-labeled C99 in lipid vesicles with different protein/lipid (mol/mol) ratios from 1:800 to 1:50. (A) Superimposed spectra (1:800, 1:400, 1:200, 1:100, and 1:50 C99/lipid) for G700R1, G704R1, G708R1, and G709R1. The overlays of the five spectra for each mutant exhibit little variation within each series. (B) Superimposed spectra (same ratios as in panel A) of the G700L and G704L mutants containing a second mutation site (to Cys) for spin labeling (S697R1). Similar to that for panel A, the superimposed spectra demonstrate little variation within each series. (C, D) EPR intensity at 3464 G was plotted as a function of the total C99 concentration and fit by a model for homodimerization.

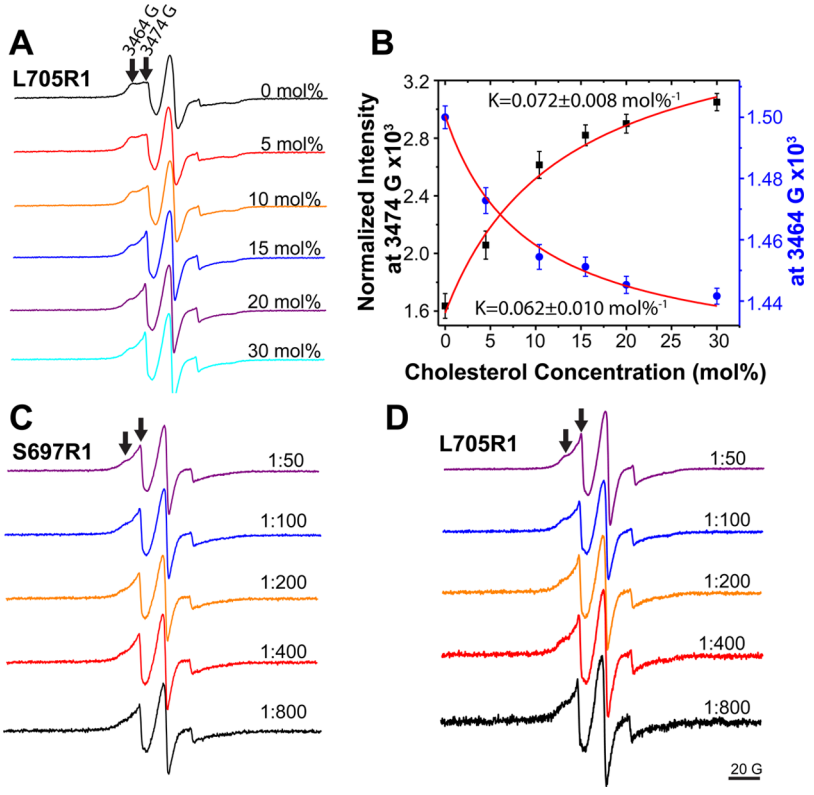

Figure 5. CW EPR spectra of C99 in the presence of cholesterol. (A) CW EPR spectra of L705R1 C99 at a protein/lipid molar ratio of 1:100 in vesicles containing cholesterol ranging from 0 to 30 mol %. All spectra were normalized (with respect to their double integrations) to the same amount of spin label. (B) EPR intensities at 3474 (right arrow) and 3464 G (left arrow) from panel A were plotted as a function of total C99 concentration and fit by a model describing the competition between the homodimerization of C99 and the 1:1 complex formation between C99 and cholesterol (eq 15). Note that the determined K describes the superequilibrium (eq 12) and is not a true dissociation or association constant. (C) CW EPR spectra of S697R1 C99 in vesicles containing 20 mol % cholesterol at protein/lipid (mol/mol) ratios varying from 1:800 to 1:50. (D) Same as in panel C except that the spin label is attached to L705C, which is located inside the membrane.

Identification of Homodimerization Interface Sites in the TMD. Most previous studies of C99 homodimerization are in agreement that the homodimerization interface of C99 is associated with the $G_{700}XXXG_{704}XXXG_{708}$ and/or

dx.doi.org/10.1021/bi400735x | *Biochemistry* 2013, 52, 5051−5064

$G_{709}XXXA_{713}$ motifs.[20,24,26,28−31,35] Therefore, we mutated sites 700−704, 705, 708, 709, and 713 to cysteine and attached spin labels. The replacement of each of the four Gly sites (700, 704, 708, and 709) with spin-labeled cysteine led to EPR spectra sets that are no longer dependent on the protein/lipid ratio (Figure 4A), indicating that these glycines are essential for homodimerization. For two of those sites (700 and 704), we also made Gly-to-Leu mutations in conjunction with spin labeling at site 697 (the EPR spectrum of which is shown to be sensitive to dimerization in Figure 1). Again, the EPR spectra were invariant with changes in the protein/lipid ratio (Figure 4). These results indicate that all three glycines in the $G_{700}XX-XG_{704}XXXG_{708}$ zipper and also Gly709 are important for homodimerization. In contrast, the replacement of Ala701, Ile702, Ile703, Leu705, and Ala713 with spin-labeled Cys showed saturable curves with increasing C99 concentration (Figure 4C,D, Supporting Information Figure S1). The fitting of these curves by the model for homodimerization results in $K_{d,dimer}$ values of 0.30 ± 0.18 (for 701), 0.34 ± 0.16 (for 702), 0.51 ± 0.15 (for 703), and 0.48 ± 0.20 mol % (for 713). These $K_{d,dimer}$ values are in the same range with each other and with wild type, indicating that these sites are not essential for homodimerization (Figure 4C,D; the data for L705 is shown in Figure 2). It is particularly interesting that mutation of Ala713 does not result in the loss of dimerization because this is the alanine in the $G_{709}XXXA_{713}$ motif. This indicates that the role of Gly709 in promoting dimerization is unrelated to Ala713.

Cholesterol Binding to Monomeric C99 Competes With the Homodimerization of the Protein. C99 was spin labeled at the L705C site in its transmembrane domain, which is a site that reports well for the oligomeric state (Figure 2) but that is not at the dimer interface. A sample was prepared with a 1:100 C99/lipid ratio where over 50% of the protein is homodimerized on the basis of the above-determined K_d for homodimerization. This is evident via the broad component seen in the top trace spectrum of Figure 5A. A series of samples were then prepared in which spin-labeled C99 was maintained at a constant mol % concentration (relative to lipid) and in which cholesterol was introduced into the membranes at different concentrations ranging from 5 to 30 mol %. This range is physiologically relevant.[36,41−43] It can be seen that the very broad dimer component of the CW EPR spectrum disappears in the course of this titration, suggestive of a cholesterol-binding-induced shift in the monomer−dimer equilibrium toward the monomer. A plot of the EPR intensity at 3474 G as a function of the cholesterol concentration (Figure 5B) exhibits a saturable curve. A model (eq 15) describing the competition between homodimerization and cholesterol binding to monomeric C99 fit very well to the data, leading to an average superequilibrium constant, K, of 0.067 ± 0.010 mol $\%^{-1}$ (Figure 5B). Using the $K_{d,dimer}$ value of 0.47 mol % determined independently above, $K_{d,chol}$ was then calculated using eq 12 to be 2.7 ± 0.8 mol %.

We next took the same two spin-labeled mutants used in the C99 titrations of Figure 2 and repeated the EPR-monitored protein/lipid ratio variation experiment in membranes that included 20 mol % cholesterol, which is a concentration that is 4-fold higher than its K_d for binding to C99 in bicelles[15] and is physiologically reasonable.[36,41−43] It can be seen that cholesterol at this level was able to reduce the homodimerization of C99 at concentrations of the protein as high as 4 times its K_d for homodimerization (Figure 5C,D).

That a competition between cholesterol binding and homodimerization takes place was confirmed by FRET measurements. Shown in Figure 6 are the FRET results for a

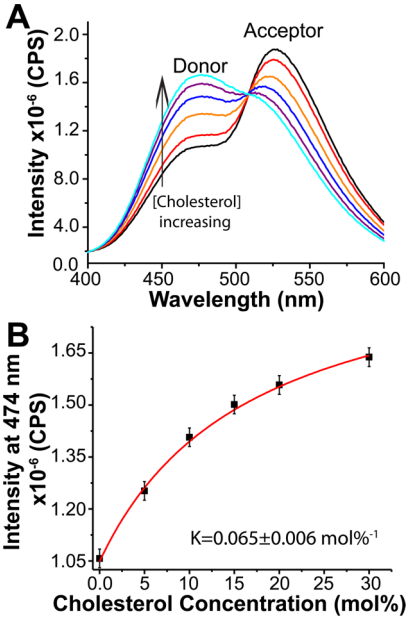

Figure 6. (A) FRET spectra of fluorescently labeled C99 S730C in lipid vesicles with a donor/acceptor ratio of 1:4 and a total C99/lipid (mol/mol) ratio of 1:100 containing different amounts of cholesterol: 0 (black), 5 (red), 10 (orange), 15 (blue), 20 (purple), and 30 mol % (cyan). (B) Intensity of the spectrum at 474 nm was plotted as a function of the cholesterol mol % and then fit by a model (eq 17) describing the competition between C99 homodimerization and 1:1 complex formation between monomeric C99 and cholesterol. (Note that 1 mol % cholesterol corresponds to 1 molecule of cholesterol for every 100 molecules of lipid and protein in the vesicles.)

1:100 C99/lipid (1 mol % C99) sample that contains a fixed ratio of FRET donor- and acceptor-labeled forms of C99. The FRET acceptor signal at ca. 525 nm has maximum intensity for a sample containing no cholesterol and then gradually decreases as the cholesterol mole fraction levels in the sample are increased, indicative of the disruption of donor−acceptor proximity by cholesterol. In Figure 5B, the intensity of the growing FRET donor signal at ca. 470 nm is plotted as a function of the cholesterol concentration. It can be seen that the intensity of the donor signal (representing the monomer) increases with increasing amounts of cholesterol. Once again, a model (eq 17) describing the competition between homodimerization and cholesterol binding fits the data well, yielding a superequilibrium constant, K, value of 0.065 ± 0.006 mol $\%^{-1}$. This leads to a K_d value of 2.6 ± 0.9 mol % for cholesterol binding to the monomer (eq 12), which is a value in excellent agreement with the value determined from the EPR data of Figure 5. Averaging the EPR result with the fluorescence result leads to the conclusion that cholesterol binds to monomeric C99 in POPC/POPG vesicles with a K_d value of 2.7 ± 0.3 mol % in a manner that is competitive with homodimerization.

DISCUSSION

Energetics of Homodimerization of C99 in Lipid Vesicles. The full-length amyloid precursor protein is thought to dimerize in a manner that is driven primarily by interactions involving its large extracellular domain.[44−48] The C99 domain

dx.doi.org/10.1021/bi400735x | Biochemistry 2013, 52, 5051−5064

($APP_{672-770}$) of APP does not appear to significantly contribute to the dimerization of the full-length protein.[28] However, it is clear from a variety of biochemical and biophysical studies of the C99 protein and its fragments that this protein does have a propensity to dimerize, although the avidity of homodimerization has not been thermodynamically quantified.[20,21,23−26,28−30,32,33,35] Of particular importance is the NMR-based determination of the structure (in dodecylphosphocholine micelles) of homodimeric $APP_{686-724}$,[30] which is a TMD-domain containing fragment of C99. This structure has interesting similarities to the NMR-based structure of the C99 monomer in lyso-phospholipid micelles.[15] In particular, both structures highlight a hinge role for the $G_{708}G_{709}$ segment in facilitating the flexible bending of the C99 TMD, as was previously proposed based on simulations.[49] The $APP_{686-724}$ dimer structure is surprising in that the transmembrane segments interact as left-handed coiled-coil helices, with the $G_{709}XXXA_{713}$ motif being central to the dimer interface. Although the possible importance of this motif in driving homodimerization had previously been proposed,[24] most earlier studies had concluded that it is the glycine zipper ($G_{700}XXXG_{704}XXXG_{708}$), particularly interactions involving the G700 and G704 sites, that drives the dimerization of C99.[20,26,28,29,31,35] There is a clear imperative to quantitate the equilibrium between the monomer and dimer forms of C99 and also to verify which residues are critical to the dimer interface. Moreover, because the biophysical and biochemical measurements made in micelles or other nonbilayered model membrane conditions are invariably subject to questions regarding the possible distortion of the results relative to more native-like bilayer conditions, it is important that these issues be addressed in lipid bilayers.

Here, we used EPR and FRET methods to interrogate the homodimerization of C99 in POPC/POPG (3:1 mol/mol) lipid vesicles at pH 6.5 and temperatures where the bilayers are in the liquid crystalline phase (L_α), which closely matches the properties of bulk-phase biological membranes. It was observed using both EPR and FRET that homodimerization occurs with a K_d value of 0.47 ± 0.15 mol %. This means that in POPC/POPG vesicles at C99 concentrations lower than 0.47 mol % (ca. 1:200 C99/lipid) the protein will be primarily monomeric, whereas the homodimer will dominate at C99 concentrations higher than 1 C99 for every 200 lipids. A K_d value of 0.47 mol % corresponds to an equilibrium free energy in favor of dimerization of only −3.2 kcal/mol. Therefore, C99 does have a propensity to dimerize in POPC/POPG vesicles but only to a modest degree. Assuming that the 0.47 mol % K_d measured for dimerization in POPC/POPG bilayers approximates the K_d value in the bulk phase of native membranes, this indicates that the homodimerization of C99 is likely to occur to a significant extent only if physiological concentrations of C99 are in the range of 1 or more C99 molecules for every ca. 200 lipids. Is such a concentration likely to ever be attained under physiological conditions? One C99 molecule per 200 lipids means the membranes would have to contain 10% or higher by weight C99. Although C99 does not seem to have been quantitated in cells, it is known that it has a much more rapid turnover rate than its full-length APP precursor; therefore, it can be assumed to have a lower concentration than APP.[50−52] APP has been purified to near homogeneity from the membrane protein fraction of brain membranes, with the reported[52,53] fold purification being in the range of 10^3−10^4. This suggests that the physiological concentration of C99 in neuronal membranes is orders of magnitude lower than 0.47 mol %. One might expect to find C99's abundance to be relatively high in the detergent-resistant (lipid raft) fraction of neuronal membranes[50] (particularly hippocampal neurons[54]), but it is clear from SDS-PAGE of this fraction (Figure 5 in ref 55) that C99 is at most only a minor component of the neuronal-raft proteome. Neurons appear to generate amyloid-β at a rate of a few molecules per second,[56] which is inconsistent with a high (>0.1 mol %) level of its C99 precursor in neuronal membranes, particularly because C99 is thought to be rapidly converted to amyloid-β. Although it cannot be absolutely ruled out that local membrane concentrations of C99 under physiological conditions ever reach the order of 0.5 mol %, this seems unlikely. It should also be noted that in cell biological studies that involve the expression of C99 in model mammalian cell lines, the concentration of the protein may often be much higher than it is under true physiological conditions. This fact should be taken into account when interpreting or designing experimental studies of C99 dimerization that involve the use of vector-based expression of this protein in model cell lines.

That C99 is rich in GXXXG motifs and yet homodimerizes with only modest affinity is not unprecedented for membrane proteins containing these motifs. For example, the homodimerization of the isolated transmembrane domains of receptor tyrosine kinases is typically weak despite the presence of GXXXG motifs.[17,57−59]

Roles of the Glycine Zipper and GXXXA Motifs in the Homodimerization of C99. The results of this work indicate a significantly reduced dimerization following the replacement of any of the three Gly sites in the $G_{700}XXXG_{704}XXXG_{708}$ zipper with spin-labeled cysteine. The same was also true for Gly_{709} in the $G_{709}XXXA_{713}$ motif. For $G_{700}XXXG_{704}$, it was previously observed that mutation of either of these glycine residues to alanine was sufficient to suppress dimerization.[15] However, the replacement of Ala713 with spin-labeled cysteine in this study had no impact on dimerization. The same is true for replacements at sites 701−703 and 705. Although our results cannot rule out the possibility that other (untested) sites in C99 contribute significantly to homodimerization, this work shows that the glycine zipper is a critical structural element, with the Gly sites on the face of the helix allowing two interacting C99 molecules to form an intimate and stabilizing interface. These results are generally consistent with previous TOXCAT, mutagenesis, and biophysical studies that concluded the Gly zipper is key for dimerization.[24,30] Possible specific structural modes consistent with a central role for the Gly zipper have previously been put forward based on computer modeling.[31,33,35] Our results are somewhat less consistent with a previous study from our lab and one other group that concluded that only the $G_{700}XXXG_{704}$ motif and not the entire zipper is important for homodimerization.[20,28]

It is interesting that Gly_{709} is important for dimerization but A_{713} is not. This disfavors the conclusions of certain previous studies that the $G_{709}XXXA_{713}$ motif is the central element of the C99 dimer.[24,30] Most striking among the previous studies is the NMR-based structure of the $APP_{686-724}$ (fragment of C99) dimer in dodecylphosphocholine micelles.[30] The disagreement of our data with that structure may reflect the very different model membrane conditions used in the NMR study (DPC micelles) compared to those in this work. Alternatively, the removal for the NMR study of most of the N-terminal ectodomain and all of the C-terminal cytosolic domain of C99

might have resulted in a different dimerization mode than that which exists for the full-length C99. This seems plausible in light of previous data that indicate C99 may adopt an alternative $G_{709}XXXA_{713}$-centric mode of dimerization if the glycine zipper is disrupted via mutagenesis,[26] although this phenomenon was not observed in this work.

Cholesterol Binding to the C99 Monomer Competes with Homodimerization. In previous work we demonstrated that cholesterol forms a 1:1 complex with monomeric C99 in dihexanoylphosphatidylcholine-dimyristoylphosphatidylcholine (DHPC-DMPC) bicelles, with an observed K_d value of 5 mol %.[15] In this work, we confirmed that cholesterol binds to C99 in bilayered POPC/POPG lipid vesicles with a K_d value of 2.7 ± 0.3 mol %, corresponding to a free energy of −2.1 kcal/mol in favor of complex formation. Moreover, this binding event was competitive with homodimerization. The fact that the binding of cholesterol to C99 in lipid vesicles is stronger than in bicelles is not surprising. Although bicelles more closely approximate membranes than do micelles, they do contain detergent and are a less-ideal membrane mimic than lipid vesicles. At membrane cholesterol concentrations higher than the 2.7 mol % value for K_d determined in this work, the majority of C99 will be in complex with cholesterol. 2.7 mol % is on the low end of the concentration range for cholesterol in the membranes of mammalian cells (especially the Golgi, plasma, and endosomal membranes).[36,41−43] Given this and in light of the fact that the concentration of C99 in native cell membranes is probably usually far below its K_d for homodimerization, the available data suggest that the most common form of C99 under physiological conditions will be a monomer in complex with cholesterol. Of course, we cannot rule out the possibility that other factors pertaining to the physiological conditions could alter the K_d values for dimerization and/or cholesterol binding; for example, the presence of other proteins that may interact with C99 and alter its monomer−dimer equilibrium.

That cholesterol binding to monomeric C99 competes with homodimerization is not surprising in light of the fact that the binding interfaces on C99 for these two types of interactions are highly overlapped. Here, we found that all four Gly sites in C99's TMD are essential for homodimerization. Previously, we showed that these very same Gly were either critical (G700 and G704) or important (G708 and G709) for cholesterol binding.[15] The remainder of the cholesterol-binding site is located in the N-terminal loop leading into the transmembrane domain, which includes the residues that form hydrogen bonds with cholesterol's hydroxyl headgroup. The 3D structure of the C99 monomer determined by NMR in LMPG micelles revealed that the three glycine residues of the zipper confer a flat surface to the face of TM helix near the ectoplasm.[15] This surface provides the basis for either an intimate homodimerization interface or for a favorable interface between C99 and the steroid-ring system of cholesterol, which is also flat and rigid. For both the homodimer− and monomer−cholesterol interfaces, van der Waals interactions should be favorable. The formation of these interfaces is also likely to be driven in part by entropy: when two flat surfaces interact with each other in a fluid phase membrane, their interface is entropically favored because the surfaces no longer have to be solvated by the normally dynamic chains of the surrounding lipids whose motions would be dampened somewhat by interacting with the rigid and flat surfaces.[60,61]

The work of this Article consolidates the notion of a bifunctional role for the key GXXXG motifs of C99 in promoting either cholesterol binding or homodimerization. In this regard, it is interesting to recognize a very recent paper by Octave and co-workers that describes an apparent role for APP and C99 in regulating the biosynthesis and turnover of cholesterol in neurons,[62] which is a paper that follows previous studies suggesting roles for the amyloidogenic pathway in regulating cellular cholesterol homeostasis (reviewed in ref 63). The Octave paper provides evidence for the direct binding of C99 and APP to sterol regulatory element binding protein 1 (SREBP1), which is a key protein in the signaling pathway that induces a transcriptional response when cellular cholesterol levels are low. The binding of C99/APP to SREBP1 suppresses this signaling pathway. Moreover, C99 was unable to bind SREBP1 when either of the Gly in the $G_{700}XXXG_{704}$ motif were mutated. It is an interesting and yet unaddressed question as to whether the mutations suppress binding because Gly700 and Gly704 are directly involved in the binding interface with SREBP1 (which would represent yet another functional role for these glycines!) or whether binding of C99 to SREBP1 is activated when C99 forms its 1:1 complex with cholesterol. The latter possibility would suggest that one function of C99 (and possibly of APP) is to directly serve as a cholesterol sensor in pathways that control cell cholesterol levels, as previously hypothesized.[20]

Dimerization of C99 and Cleavage by γ-Secretase. There has been much interest in the oligomeric state of γ-secretase and the question of how it relates to the oligomeric state of C99. The γ-secretase complex is composed of four different integral membrane proteins, of which presenilin is the catalytic subunit. A number of early reports suggested that the γ-secretase complex forms dimers or higher oligomers.[64−66] However, recent medium-resolution cryo-EM results and related biochemical studies appear to clearly demonstrate that the complex is both monomeric and active.[67−69] In addition, the recently published crystal structure of an archaebacterial homologue of presenilin shows that although this enzyme crystallizes as a homotetramer, each subunit appears to contain its own active site located on the far side of the transmembrane domain from the fourfold symmetry axis.[70] These studies disfavor the notions that the active site of γ-secretase is composed of residues from more than one subunit and that the active sites on adjacent subunits could be sufficiently proximal such that both components of a C99 dimer can simultaneously occupy adjacent active sites without disrupting the homodimer contacts.

γ-Secretase does appear to be able to cleave both dimeric and monomeric substrates.[22,34] On the one hand, disulfide-linked C99 homodimers have been shown to be cleaved to generate disulfide-bonded amyloid-β dimers.[34] On the other hand, mutations of the Gly residues critical for the weak homodimerization of C99 do not dramatically reduce the overall γ-secretase processing of C99, although these mutations do alter the distribution of amyloid-β peptides that are generated.[26,28] It has been proposed that γ-secretase has a substrate docking site that is located next to the active site. Therefore, it seems possible that the enzyme may be able to bind one C99 molecule at its active site and a second at the docking site.[71−74] Whether the Gly zipper-associated homodimerization interface of C99 could be maintained with one subunit at the active site and the other at the docking site is not yet clear. It is important to note that γ-secretase has many other

dx.doi.org/10.1021/bi400735x | Biochemistry 2013, 52, 5051−5064

single-span membrane protein substrates and many do not have a Gly zipper, GXXXG-class motifs, or a known propensity to homodimerize.[75] It is also revealing that in studies of a NOTCH chimera in which its normal transmembrane domain was replaced with that of avidly homodimerizing glycophorin A, the version of the chimera with the wild-type glycophorin A sequence was processed by γ-secretase significantly less efficiently than a mutant form in which the GXXXG motif was disrupted.[76] Another study also concluded that the possible homodimerization of the NOTCH TMD is unrelated to its cleavage by γ-secretase.[77] Our conclusion in this Article that C99 dimerizes with only modest affinity and may have little tendency to form dimers at physiological concentrations does not conflict with what is currently believed about its interactions with γ-secretase.

Cholesterol Binding by C99 and Cleavage by γ-Secretase. There is considerable evidence that elevated levels of cholesterol promote the amyloidogenic pathway, resulting in increased levels of amyloid-β production.[5−14] How might cholesterol binding to C99 explain this phenomenon?

This work confirms our previous suggestion that C99 will be very often complexed with cholesterol under physiological conditions.[15] We have previously hypothesized that this complex (and the corresponding complex of cholesterol with full-length APP) may promote amyloidogenesis by increasing the partitioning of C99 and APP into cholesterol-rich membrane domains known as lipid rafts.[15,20] This would promote the formation of amyloid-β because, as reviewed elsewhere, there is much evidence that β- and γ-secretase preferentially associate with rafts.[78−83]

A second possible mechanism by which cholesterol binding to C99 could promote amyloid-β formation is by directly promoting C99 binding to γ-secretase (to either the putative docking site or the active site or both) and its subsequent cleavage. Studies with purified γ-secretase that has been reconstituted into lipid vesicles have shown a 2- to 4-fold enhancement in the rates of production of both $A\beta_{40}$ and $A\beta_{42}$ by the presence of cholesterol in the membranes, with optimal levels of cholesterol being in the range of 5−20 mol %, depending on vesicle composition.[67] It is possible that the rate increase may simply reflect the impact of membrane cholesterol on γ-secretase function as a result of the effect of cholesterol on bulk membrane properties and/or direct interactions with the enzyme.[84−86] However, it is interesting that the maximally activating levels of cholesterol correspond to concentrations at which the near saturation of cholesterol binding to C99 is expected on the basis of the K_d value of 2.7 mol % determined in this work. One wonders if cholesterol could remain associated with C99 at the γ-secretase substrate docking site and/or in the active site. The glycine zipper of C99 is associated with empty space on the flat Gly-rich face of the transmembrane helix that is normally occupied by non-Gly amino acid side chains in most other γ-secretase substrates.[75] This suggests the possibility of a cleft between the face of the C99 Gly zipper and the γ-secretase side chains at the binding site. The questions of whether such a cleft is present following C99 binding, whether cholesterol could remain bound in such a cleft, and how this would impact the cleavage of C99 may be worthy of future investigation.

Cholesterol may under some conditions compete with γ-secretase modulators (GSMs) for binding to C99 when bound to γ-secretase. GSMs are small molecules that modulate the cleavage of C99 by γ-secretase to alter the ratio between the short forms of amyloid-β and the more pathogenic long forms.[87,88] GSM action is C99-selective in the sense that the cleavage of other γ-secretase substrates is not impacted. Although there has been controversy as to whether GSMs can bind directly to free C99,[21,32,89−91] most of the recent evidence suggests that GSMs act by forming a ternary complex with C99 and γ-secretase.[87,88,92−96] Remarkably, there are a couple of reports that a mutation of the Gly in the zipper motif of C99 results in the elimination of GSM action, suggesting that the face of the zipper may interact directly with GSMs in ternary complexes with γ-secretase.[91,97] Although this is not without contention,[98] it seems plausible that the cleft between the face of the C99 Gly zipper and the surrounding γ-secretase residues (hypothesized above) might represent the GSM binding site. Whether GSMs might compete with cholesterol for C99-mediated binding to γ-secretase is an interesting possibility that may be worthy of future testing.

Finally, we note the possibility that cholesterol might also bind to full-length APP and promote its amyloidogenic cleavage by β-secretase through mechanisms analogous to those outlined herein for C99 and γ-secretase. The structure and membrane interactions of the C99 domain of full-length APP is likely to be similar to the structure of isolated C99 such that cholesterol binding to APP is likely to be of similar affinity as it is for C99. Moreover, there are persistent reports that β-secretase is also found to be enriched in cholesterol-rich membrane domains (reviewed in refs 78 and 81).

CONCLUSIONS

This work extends recent studies by showing that cholesterol binds to C99 in bilayered lipid vesicles in a manner that is competitive with homodimerization and by confirming the observations made in bicellar model membranes that the dissociation constant is well within the physiological concentration range of cholesterol in mammalian cells (Figure 7). We also found that the quantitative homodimerization affinity of C99 is modest to the point where it is difficult to argue that dimerization is likely to be physiologically relevant. However, C99 forms a 1:1 complex with cholesterol that appears to be of clear physiological relevance. This raises questions for future study regarding the significance of this binding event for C99 function, membrane trafficking, and amyloidogenic proteolytic processing. Finally, we note that the involvement of the glycine zipper in the C99 TMD in cholesterol binding, homodimerization, and interactions with GSMs (in the C99/γ-secretase complex) suggests an extraordinary importance for this motif; the possession of which sets C99 apart from most other γ-secretase substrates.

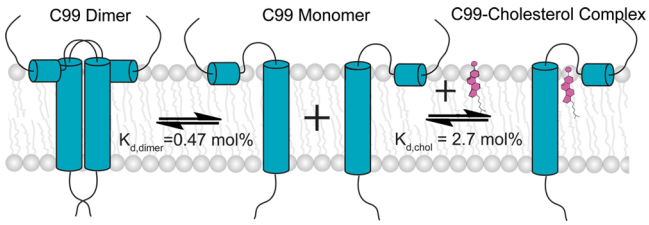

Figure 7. Competition between homodimerization and cholesterol binding to free C99 in lipid vesicles. The K_d values were determined in this work.

dx.doi.org/10.1021/bi400735x | *Biochemistry* 2013, 52, 5051−5064

■ ASSOCIATED CONTENT

Supporting Information

Dependence of the EPR spectra from C99 that is spin labeled at sites 701, 702, and 713 on the protein mol % in vesicles. This material is available free of charge via the Internet at http://pubs.acs.org.

■ AUTHOR INFORMATION

Corresponding Author

*Tel: 615-936-3756. Fax: 615-936-2211. E-mail: chuck.sanders@vanderbilt.edu.

Funding

This work was supported by NIH grants RO1 GM106672 and PO1 GM080513.

Notes

The authors declare no competing financial interest.

■ ACKNOWLEDGMENTS

We thank Arina Hadziselimovic for technical assistance, Brett Kroncke for proofreading, and Paul Barrett for many helpful discussions.

■ REFERENCES

(1) De, S. B., Vassar, R., and Golde, T. (2010) The secretases: enzymes with therapeutic potential in Alzheimer disease. *Nat. Rev. Neurol. 6*, 99−107.

(2) Hardy, J. (2009) The amyloid hypothesis for Alzheimer's disease: a critical reappraisal. *J. Neurochem. 110*, 1129−1134.

(3) Selkoe, D. J. (2011) Alzheimer's disease. *Cold Spring Harbor Perspect. Biol. 3*, a004457-1−a004457-16.

(4) Teich, A. F., and Arancio, O. (2012) Is the amyloid hypothesis of Alzheimer's disease therapeutically relevant? *Biochem. J. 446*, 165−177.

(5) Bodovitz, S., and Klein, W. L. (1996) Cholesterol modulates alpha-secretase cleavage of amyloid precursor protein. *J. Biol. Chem. 271*, 4436−4440.

(6) Fonseca, A. C., Resende, R., Oliveira, C. R., and Pereira, C. M. (2010) Cholesterol and statins in Alzheimer's disease: current controversies. *Exp. Neurol. 223*, 282−293.

(7) Grimm, M. O., Grimm, H. S., Tomic, I., Beyreuther, K., Hartmann, T., and Bergmann, C. (2008) Independent inhibition of Alzheimer disease beta- and gamma-secretase cleavage by lowered cholesterol levels. *J. Biol. Chem. 283*, 11302−11311.

(8) Guardia-Laguarta, C., Coma, M., Pera, M., Clarimon, J., Sereno, L., Agullo, J. M., Molina-Porcel, L., Gallardo, E., Deng, A., Berezovska, O., Hyman, B. T., Blesa, R., Gomez-Isla, T., and Lleo, A. (2009) Mild cholesterol depletion reduces amyloid-beta production by impairing APP trafficking to the cell surface. *J. Neurochem. 110*, 220−230.

(9) Kojro, E., Gimpl, G., Lammich, S., Marz, W., and Fahrenholz, F. (2001) Low cholesterol stimulates the nonamyloidogenic pathway by its effect on the alpha -secretase ADAM 10. *Proc. Natl. Acad. Sci. U.S.A. 98*, 5815−5820.

(10) Simons, M., Keller, P., De, S. B., Beyreuther, K., Dotti, C. G., and Simons, K. (1998) Cholesterol depletion inhibits the generation of beta-amyloid in hippocampal neurons. *Proc. Natl. Acad. Sci. U.S.A. 95*, 6460−6464.

(11) Wahrle, S., Das, P., Nyborg, A. C., McLendon, C., Shoji, M., Kawarabayashi, T., Younkin, L. H., Younkin, S. G., and Golde, T. E. (2002) Cholesterol-dependent gamma-secretase activity in buoyant cholesterol-rich membrane microdomains. *Neurobiol. Dis. 9*, 11−23.

(12) Fassbender, K., Simons, M., Bergmann, C., Stroick, M., Lutjohann, D., Keller, P., Runz, H., Kuhl, S., Bertsch, T., von Bergmann, K., Hennerici, M., Beyreuther, K., and Hartmann, T. (2001) Simvastatin strongly reduces levels of Alzheimer's disease beta -amyloid peptides Abeta 42 and Abeta 40 in vitro and in vivo. *Proc. Natl. Acad. Sci. U.S.A. 98*, 5856−5861.

(13) Refolo, L. M., Pappolla, M. A., LaFrancois, J., Malester, B., Schmidt, S. D., Thomas-Bryant, T., Tint, G. S., Wang, R., Mercken, M., Petanceska, S. S., and Duff, K. E. (2001) A cholesterol-lowering drug reduces beta-amyloid pathology in a transgenic mouse model of Alzheimer's disease. *Neurobiol. Dis. 8*, 890−899.

(14) Runz, H., Rietdorf, J., Tomic, I., de Bernard, M., Beyreuther, K., Pepperkok, R., and Hartmann, T. (2002) Inhibition of intracellular cholesterol transport alters presenilin localization and amyloid precursor protein processing in neuronal cells. *J. Neurosci. 22*, 1679−1689.

(15) Barrett, P. J., Song, Y., Van Horn, W. D., Hustedt, E. J., Schafer, J. M., Hadziselimovic, A., Beel, A. J., and Sanders, C. R. (2012) The amyloid precursor protein has a flexible transmembrane domain and binds cholesterol. *Science 336*, 1168−1171.

(16) Kim, S., Jeon, T. J., Oberai, A., Yang, D., Schmidt, J. J., and Bowie, J. U. (2005) Transmembrane glycine zippers: physiological and pathological roles in membrane proteins. *Proc. Natl. Acad. Sci. U.S.A. 102*, 14278−14283.

(17) MacKenzie, K. R., and Fleming, K. G. (2008) Association energetics of membrane spanning alpha-helices. *Curr. Opin. Struct. Biol. 18*, 412−419.

(18) Senes, A., Gerstein, M., and Engelman, D. M. (2000) Statistical analysis of amino acid patterns in transmembrane helices: the GxxxG motif occurs frequently and in association with beta-branched residues at neighboring positions. *J. Mol. Biol. 296*, 921−936.

(19) Kleiger, G., Grothe, R., Mallick, P., and Eisenberg, D. (2002) GXXXG and AXXXA: common alpha-helical interaction motifs in proteins, particularly in extremophiles. *Biochemistry 41*, 5990−5997.

(20) Beel, A. J., Mobley, C. K., Kim, H. J., Tian, F., Hadziselimovic, A., Jap, B., Prestegard, J. H., and Sanders, C. R. (2008) Structural studies of the transmembrane C-terminal domain of the amyloid precursor protein (APP): does APP function as a cholesterol sensor? *Biochemistry 47*, 9428−9446.

(21) Botev, A., Munter, L. M., Wenzel, R., Richter, L., Althoff, V., Ismer, J., Gerling, U., Weise, C., Koksch, B., Hildebrand, P. W., Bittl, R., and Multhaup, G. (2011) The amyloid precursor protein C-terminal fragment C100 occurs in monomeric and dimeric stable conformations and binds gamma-secretase modulators. *Biochemistry 50*, 828−835.

(22) Eggert, S., Midthune, B., Cottrell, B., and Koo, E. H. (2009) Induced dimerization of the amyloid precursor protein leads to decreased amyloid-beta protein production. *J. Biol. Chem. 284*, 28943−28952.

(23) Goo, J. H., and Park, W. J. (2004) Elucidation of the interactions between C99, presenilin, and nicastrin by the split-ubiquitin assay. *DNA Cell Biol. 23*, 59−65.

(24) Gorman, P. M., Kim, S., Guo, M., Melnyk, R. A., McLaurin, J., Fraser, P. E., Bowie, J. U., and Chakrabartty, A. (2008) Dimerization of the transmembrane domain of amyloid precursor proteins and familial Alzheimer's disease mutants. *BMC Neurosci. 9*, 17.

(25) Khalifa, N. B., Van, H. J., Tasiaux, B., Huysseune, S., Smith, S. O., Constantinescu, S. N., Octave, J. N., and Kienlen-Campard, P. (2010) What is the role of amyloid precursor protein dimerization? *Cell Adhes. Migr. 4*, 268−272.

(26) Kienlen-Campard, P., Tasiaux, B., Van, H. J., Li, M., Huysseune, S., Sato, T., Fei, J. Z., Aimoto, S., Courtoy, P. J., Smith, S. O., Constantinescu, S. N., and Octave, J. N. (2008) Amyloidogenic processing but not amyloid precursor protein (APP) intracellular C-terminal domain production requires a precisely oriented APP dimer assembled by transmembrane GXXXG motifs. *J. Biol. Chem. 283*, 7733−7744.

(27) Mao, G., Tan, J., Cui, M. Z., Chui, D., and Xu, X. (2009) The GxxxG motif in the transmembrane domain of AbetaPP plays an essential role in the interaction of CTF beta with the gamma-secretase complex and the formation of amyloid-beta. *J. Alzheimer's Dis. 18*, 167−176.

(28) Munter, L. M., Voigt, P., Harmeier, A., Kaden, D., Gottschalk, K. E., Weise, C., Pipkorn, R., Schaefer, M., Langosch, D., and Multhaup, G. (2007) GxxxG motifs within the amyloid precursor protein

transmembrane sequence are critical for the etiology of Abeta42. *EMBO J. 26*, 1702−1712.
(29) Munter, L. M., Botev, A., Richter, L., Hildebrand, P. W., Althoff, V., Weise, C., Kaden, D., and Multhaup, G. (2010) Aberrant amyloid precursor protein (APP) processing in hereditary forms of Alzheimer disease caused by APP familial Alzheimer disease mutations can be rescued by mutations in the APP GxxxG motif. *J. Biol. Chem. 285*, 21636−21643.
(30) Nadezhdin, K. D., Bocharova, O. V., Bocharov, E. V., and Arseniev, A. S. (2012) Dimeric structure of transmembrane domain of amyloid precursor protein in micellar environment. *FEBS Lett. 586*, 1687−1692.
(31) Pester, O., Barrett, P. J., Hornburg, D., Hornburg, P., Probstle, R., Widmaier, S., Kutzner, C., Durrbaum, M., Kapurniotu, A., Sanders, C. R., Scharnagl, C., and Langosch, D. (2013) The backbone dynamics of the amyloid precursor protein transmembrane helix provides a rationale for the sequential cleavage mechanism of gamma-secretase. *J. Am. Chem. Soc. 135*, 1317−1329.
(32) Richter, L., Munter, L. M., Ness, J., Hildebrand, P. W., Dasari, M., Unterreitmeier, S., Bulic, B., Beyermann, M., Gust, R., Reif, B., Weggen, S., Langosch, D., and Multhaup, G. (2010) Amyloid beta 42 peptide (Abeta42)-lowering compounds directly bind to Abeta and interfere with amyloid precursor protein (APP) transmembrane dimerization. *Proc. Natl. Acad. Sci. U.S.A. 107*, 14597−14602.
(33) Sato, T., Tang, T. C., Reubins, G., Fei, J. Z., Fujimoto, T., Kienlen-Campard, P., Constantinescu, S. N., Octave, J. N., Aimoto, S., and Smith, S. O. (2009) A helix-to-coil transition at the epsilon-cut site in the transmembrane dimer of the amyloid precursor protein is required for proteolysis. *Proc. Natl. Acad. Sci. U.S.A. 106*, 1421−1426.
(34) Scheuermann, S., Hambsch, B., Hesse, L., Stumm, J., Schmidt, C., Beher, D., Bayer, T. A., Beyreuther, K., and Multhaup, G. (2001) Homodimerization of amyloid precursor protein and its implication in the amyloidogenic pathway of Alzheimer's disease. *J. Biol. Chem. 276*, 33923−33929.
(35) Wang, H., Barreyro, L., Provasi, D., Djemil, I., Torres-Arancivia, C., Filizola, M., and Ubarretxena-Belandia, I. (2011) Molecular determinants and thermodynamics of the amyloid precursor protein transmembrane domain implicated in Alzheimer's disease. *J. Mol. Biol. 408*, 879−895.
(36) van Meer, G., Voelker, D. R., and Feigenson, G. W. (2008) Membrane lipids: where they are and how they behave. *Nat. Rev. Mol. Cell Biol. 9*, 112−124.
(37) Antoniou, C., Lam, V. Q., and Fung, L. W. (2008) Conformational changes at the tetramerization site of erythroid alpha-spectrin upon binding beta-spectrin: a spin label EPR study. *Biochemistry 47*, 10765−10772.
(38) Liao, H., Ellena, J., Liu, L., Szabo, G., Cafiso, D., and Castle, D. (2007) Secretory carrier membrane protein SCAMP2 and phosphatidylinositol 4,5-bisphosphate interactions in the regulation of dense core vesicle exocytosis. *Biochemistry 46*, 10909−10920.
(39) Lu, J. X., Yau, W. M., and Tycko, R. (2011) Evidence from solid-state NMR for nonhelical conformations in the transmembrane domain of the amyloid precursor protein. *Biophys. J. 100*, 711−719.
(40) White, S. H., and Wimley, W. C. (1999) Membrane protein folding and stability: physical principles. *Annu. Rev. Biophys. Biomol. Struct. 28*, 319−365.
(41) Calderon, R. O., Attema, B., and DeVries, G. H. (1995) Lipid composition of neuronal cell bodies and neurites from cultured dorsal root ganglia. *J. Neurochem. 64*, 424−429.
(42) Calderon, R. O., and DeVries, G. H. (1997) Lipid composition and phospholipid asymmetry of membranes from a Schwann cell line. *J. Neurosci. Res. 49*, 372−380.
(43) Wood, W. G., Cornwell, M., and Williamson, L. S. (1989) High performance thin-layer chromatography and densitometry of synaptic plasma membrane lipids. *J. Lipid Res. 30*, 775−779.
(44) Gralle, M., and Ferreira, S. T. (2007) Structure and functions of the human amyloid precursor protein: the whole is more than the sum of its parts. *Prog. Neurobiol. 82*, 11−32.
(45) Kaden, D., Munter, L. M., Reif, B., and Multhaup, G. (2012) The amyloid precursor protein and its homologues: structural and functional aspects of native and pathogenic oligomerization. *Eur. J. Cell Biol. 91*, 234−239.
(46) Lee, S., Xue, Y., Hu, J., Wang, Y., Liu, X., Demeler, B., and Ha, Y. (2011) The E2 domains of APP and APLP1 share a conserved mode of dimerization. *Biochemistry 50*, 5453−5464.
(47) Devauges, V., Marquer, C., Lecart, S., Cossec, J. C., Potier, M. C., Fort, E., Suhling, K., and Leveque-Fort, S. (2012) Homodimerization of amyloid precursor protein at the plasma membrane: a homoFRET study by time-resolved fluorescence anisotropy imaging. *PLoS One 7*, e44434-1−e44434-12.
(48) Gralle, M., Botelho, M. G., and Wouters, F. S. (2009) Neuroprotective secreted amyloid precursor protein acts by disrupting amyloid precursor protein dimers. *J. Biol. Chem. 284*, 15016−15025.
(49) Miyashita, N., Straub, J. E., and Thirumalai, D. (2009) Structures of beta-amyloid peptide 1−40, 1−42, and 1−55-the 672−726 fragment of APP-in a membrane environment with implications for interactions with gamma-secretase. *J. Am. Chem. Soc. 131*, 17843−17852.
(50) Cordy, J. M., Hussain, I., Dingwall, C., Hooper, N. M., and Turner, A. J. (2003) Exclusively targeting beta-secretase to lipid rafts by GPI-anchor addition up-regulates beta-site processing of the amyloid precursor protein. *Proc. Natl. Acad. Sci. U.S.A. 100*, 11735−11740.
(51) Abramowski, D., Wiederhold, K. H., Furrer, U., Jaton, A. L., Neuenschwander, A., Runser, M. J., Danner, S., Reichwald, J., Ammaturo, D., Staab, D., Stoeckli, M., Rueeger, H., Neumann, U., and Staufenbiel, M. (2008) Dynamics of Abeta turnover and deposition in different beta-amyloid precursor protein transgenic mouse models following gamma-secretase inhibition. *J. Pharmacol. Exp. Ther. 327*, 411−424.
(52) Potempska, A., Styles, J., Mehta, P., Kim, K. S., and Miller, D. L. (1991) Purification and tissue level of the beta-amyloid peptide precursor of rat brain. *J. Biol. Chem. 266*, 8464−8469.
(53) de La Fournière-Bessueille, L., Grange, D., and Buchet, R. (1997) Purification and spectroscopic characterization of beta-amyloid precursor protein from porcine brains. *Eur. J. Biochem. 250*, 705−711.
(54) Guo, Q., Li, H., Gaddam, S. S., Justice, N. J., Robertson, C. S., and Zheng, H. (2012) Amyloid precursor protein revisited: neuron-specific expression and highly stable nature of soluble derivatives. *J. Biol. Chem. 287*, 2437−2445.
(55) Williamson, R., Thompson, A. J., Abu, M., Hye, A., Usardi, A., Lynham, S., Anderton, B. H., and Hanger, D. P. (2010) Isolation of detergent resistant microdomains from cultured neurons: detergent dependent alterations in protein composition. *BMC Neurosci. 11*, 120-1−120-12.
(56) Moghekar, A., Rao, S., Li, M., Ruben, D., Mammen, A., Tang, X., and O'Brien, R. J. (2011) Large quantities of Abeta peptide are constitutively released during amyloid precursor protein metabolism in vivo and in vitro. *J. Biol. Chem. 286*, 15989−15997.
(57) Kobus, F. J., and Fleming, K. G. (2005) The GxxxG-containing transmembrane domain of the CCK4 oncogene does not encode preferential self-interactions. *Biochemistry 44*, 1464−1470.
(58) Stanley, A. M., and Fleming, K. G. (2005) The transmembrane domains of ErbB receptors do not dimerize strongly in micelles. *J. Mol. Biol. 347*, 759−772.
(59) Li, E., and Hristova, K. (2010) Receptor tyrosine kinase transmembrane domains: function, dimer structure and dimerization energetics. *Cell Adhes. Migr. 4*, 249−254.
(60) Popot, J. L., and Engelman, D. M. (2000) Helical membrane protein folding, stability, and evolution. *Annu. Rev. Biochem. 69*, 881−922.
(61) Helms, V. (2002) Attraction within the membrane. Forces behind transmembrane protein folding and supramolecular complex assembly. *EMBO Rep. 3*, 1133−1138.
(62) Pierrot, N., Tyteca, D., D'Auria, L., Dewachter, I., Gailly, P., Hendrickx, A., Tasiaux, B., Haylani, L. E., Muls, N., N'Kuli, F., Laquerriere, A., Demoulin, J. B., Campion, D., Brion, J. P., Courtoy, P.

J., Kienlen-Campard, P., and Octave, J. N. (2013) Amyloid precursor protein controls cholesterol turnover needed for neuronal activity. *EMBO Mol. Med. 5*, 608−625.
(63) Grimm, M. O., Rothhaar, T. L., and Hartmann, T. (2012) The role of APP proteolytic processing in lipid metabolism. *Exp. Brain Res. 217*, 365−375.
(64) Cervantes, S., Saura, C. A., Pomares, E., Gonzalez-Duarte, R., and Marfany, G. (2004) Functional implications of the presenilin dimerization: reconstitution of gamma-secretase activity by assembly of a catalytic site at the dimer interface of two catalytically inactive presenilins. *J. Biol. Chem. 279*, 36519−36529.
(65) Clarke, E. E., Churcher, I., Ellis, S., Wrigley, J. D., Lewis, H. D., Harrison, T., Shearman, M. S., and Beher, D. (2006) Intra- or intercomplex binding to the gamma-secretase enzyme. A model to differentiate inhibitor classes. *J. Biol. Chem. 281*, 31279−31289.
(66) Schroeter, E. H., Ilagan, M. X., Brunkan, A. L., Hecimovic, S., Li, Y. M., Xu, M., Lewis, H. D., Saxena, M. T., De, S. B., Coonrod, A., Tomita, T., Iwatsubo, T., Moore, C. L., Goate, A., Wolfe, M. S., Shearman, M., and Kopan, R. (2003) A presenilin dimer at the core of the gamma-secretase enzyme: insights from parallel analysis of Notch 1 and APP proteolysis. *Proc. Natl. Acad. Sci. U.S.A. 100*, 13075−13080.
(67) Osenkowski, P., Ye, W., Wang, R., Wolfe, M. S., and Selkoe, D. J. (2008) Direct and potent regulation of gamma-secretase by its lipid microenvironment. *J. Biol. Chem. 283*, 22529−22540.
(68) Renzi, F., Zhang, X., Rice, W. J., Torres-Arancivia, C., Gomez-Llorente, Y., Diaz, R., Ahn, K., Yu, C., Li, Y. M., Sisodia, S. S., and Ubarretxena-Belandia, I. (2011) Structure of gamma-secretase and its trimeric pre-activation intermediate by single-particle electron microscopy. *J. Biol. Chem. 286*, 21440−21449.
(69) Sato, T., Diehl, T. S., Narayanan, S., Funamoto, S., Ihara, Y., De, S. B., Steiner, H., Haass, C., and Wolfe, M. S. (2007) Active gamma-secretase complexes contain only one of each component. *J. Biol. Chem. 282*, 33985−33993.
(70) Li, X., Dang, S., Yan, C., Gong, X., Wang, J., and Shi, Y. (2013) Structure of a presenilin family intramembrane aspartate protease. *Nature 493*, 56−61.
(71) Li, H., Wolfe, M. S., and Selkoe, D. J. (2009) Toward structural elucidation of the gamma-secretase complex. *Structure 17*, 326−334.
(72) Imamura, Y., Umezawa, N., Osawa, S., Shimada, N., Higo, T., Yokoshima, S., Fukuyama, T., Iwatsubo, T., Kato, N., Tomita, T., and Higuchi, T. (2013) Effect of helical conformation and side chain structure on gamma-secretase inhibition by beta-peptide foldamers: insight into substrate recognition. *J. Med. Chem. 56*, 1443−1454.
(73) Kornilova, A. Y., Bihel, F., Das, C., and Wolfe, M. S. (2005) The initial substrate-binding site of gamma-secretase is located on presenilin near the active site. *Proc. Natl. Acad. Sci. U.S.A. 102*, 3230−3235.
(74) Watanabe, N., Image, I., II, Takagi, S., Image, I., II, Tominaga, A., Image, I., I, Tomita, T., Image, I., II, Iwatsubo, T., and Image, I., I. (2010) Functional analysis of the transmembrane domains of presenilin 1: participation of transmembrane domains 2 and 6 in the formation of initial substrate-binding site of gamma-secretase. *J. Biol. Chem. 285*, 19738−19746.
(75) Beel, A. J., and Sanders, C. R. (2008) Substrate specificity of gamma-secretase and other intramembrane proteases. *Cell. Mol. Life Sci. 65*, 1311−1334.
(76) Vooijs, M., Schroeter, E. H., Pan, Y., Blandford, M., and Kopan, R. (2004) Ectodomain shedding and intramembrane cleavage of mammalian Notch proteins is not regulated through oligomerization. *J. Biol. Chem. 279*, 50864−50873.
(77) Struhl, G., and Adachi, A. (2000) Requirements for presenilin-dependent cleavage of notch and other transmembrane proteins. *Mol. Cell 6*, 625−636.
(78) Beel, A. J., Sakakura, M., Barrett, P. J., and Sanders, C. R. (2010) Direct binding of cholesterol to the amyloid precursor protein: An important interaction in lipid-Alzheimer's disease relationships? *Biochim. Biophys. Acta 1801*, 975−982.
(79) Cheng, H., Vetrivel, K. S., Gong, P., Meckler, X., Parent, A., and Thinakaran, G. (2007) Mechanisms of disease: new therapeutic strategies for Alzheimer's disease–targeting APP processing in lipid rafts. *Nat. Clin. Pract. Neurol. 3*, 374−382.
(80) Di, P. G., and Kim, T. W. (2011) Linking lipids to Alzheimer's disease: cholesterol and beyond. *Nat. Rev. Neurosci. 12*, 284−296.
(81) Hicks, D. A., Nalivaeva, N. N., and Turner, A. J. (2012) Lipid rafts and Alzheimer's disease: protein-lipid interactions and perturbation of signaling. *Front. Membr. Physiol. Biophys. 3*, 189−207.
(82) Martins, I. J., Berger, T., Sharman, M. J., Verdile, G., Fuller, S. J., and Martins, R. N. (2009) Cholesterol metabolism and transport in the pathogenesis of Alzheimer's disease. *J. Neurochem. 111*, 1275−1308.
(83) Rushworth, J. V., and Hooper, N. M. (2010) Lipid Rafts: linking alzheimer's amyloid-beta production, aggregation, and toxicity at neuronal membranes. *Int. J. Alzheimer's Dis. 2011*, 603052.
(84) Fraering, P. C., Ye, W., Strub, J. M., Dolios, G., LaVoie, M. J., Ostaszewski, B. L., van, D. A., Wang, R., Selkoe, D. J., and Wolfe, M. S. (2004) Purification and characterization of the human gamma-secretase complex. *Biochemistry 43*, 9774−9789.
(85) Wrigley, J. D., Schurov, I., Nunn, E. J., Martin, A. C., Clarke, E. E., Ellis, S., Bonnert, T. P., Shearman, M. S., and Beher, D. (2005) Functional overexpression of gamma-secretase reveals protease-independent trafficking functions and a critical role of lipids for protease activity. *J. Biol. Chem. 280*, 12523−12535.
(86) Holmes, O., Paturi, S., Ye, W., Wolfe, M. S., and Selkoe, D. J. (2012) Effects of membrane lipids on the activity and processivity of purified gamma-secretase. *Biochemistry 51*, 3565−3575.
(87) Bulic, B., Ness, J., Hahn, S., Rennhack, A., Jumpertz, T., and Weggen, S. (2011) Chemical biology, molecular mechanism and clinical perspective of gamma-secretase modulators in alzheimer's disease. *Curr. Neuropharmacol. 9*, 598−622.
(88) Wolfe, M. S. (2012) Gamma-secretase inhibitors and modulators for Alzheimer's disease. *J. Neurochem. 120*, 89−98.
(89) Barrett, P. J., Sanders, C. R., Kaufman, S. A., Michelsen, K., and Jordan, J. B. (2011) NSAID-based gamma-secretase modulators do not bind to the amyloid-beta polypeptide. *Biochemistry 50*, 10328−10342.
(90) Beel, A. J., Barrett, P., Schnier, P. D., Hitchcock, S. A., Bagal, D., Sanders, C. R., and Jordan, J. B. (2009) Nonspecificity of binding of gamma-secretase modulators to the amyloid precursor protein. *Biochemistry 48*, 11837−11839.
(91) Kukar, T. L., Ladd, T. B., Bann, M. A., Fraering, P. C., Narlawar, R., Maharvi, G. M., Healy, B., Chapman, R., Welzel, A. T., Price, R. W., Moore, B., Rangachari, V., Cusack, B., Eriksen, J., Jansen-West, K., Verbeeck, C., Yager, D., Eckman, C., Ye, W., Sagi, S., Cottrell, B. A., Torpey, J., Rosenberry, T. L., Fauq, A., Wolfe, M. S., Schmidt, B., Walsh, D. M., Koo, E. H., and Golde, T. E. (2008) Substrate-targeting gamma-secretase modulators. *Nature 453*, 925−929.
(92) Crump, C. J., Fish, B. A., Castro, S. V., Chau, D. M., Gertsik, N., Ahn, K., Stiff, C., Pozdnyakov, N., Bales, K. R., Johnson, D. S., and Li, Y. M. (2011) Piperidine acetic acid based gamma-secretase modulators directly bind to presenilin-1. *ACS Chem. Neurosci. 2*, 705−710.
(93) Jumpertz, T., Rennhack, A., Ness, J., Baches, S., Pietrzik, C. U., Bulic, B., and Weggen, S. (2012) Presenilin is the molecular target of acidic gamma-secretase modulators in living cells. *PLoS One 7*, e30484-1−e30484-9.
(94) Ohki, Y., Higo, T., Uemura, K., Shimada, N., Osawa, S., Berezovska, O., Yokoshima, S., Fukuyama, T., Tomita, T., and Iwatsubo, T. (2011) Phenylpiperidine-type gamma-secretase modulators target the transmembrane domain 1 of presenilin 1. *EMBO J. 30*, 4815−4824.
(95) Shelton, C. C., Zhu, L., Chau, D., Yang, L., Wang, R., Djaballah, H., Zheng, H., and Li, Y. M. (2009) Modulation of gamma-secretase specificity using small molecule allosteric inhibitors. *Proc. Natl. Acad. Sci. U.S.A. 106*, 20228−20233.
(96) Zettl, H., Weggen, S., Schneider, P., and Schneider, G. (2010) Exploring the chemical space of gamma-secretase modulators. *Trends Pharmacol. Sci. 31*, 402−410.
(97) Sagi, S. A., Lessard, C. B., Winden, K. D., Maruyama, H., Koo, J. C., Weggen, S., Kukar, T. L., Golde, T. E., and Koo, E. H. (2011) Substrate sequence influences gamma-secretase modulator activity,

role of the transmembrane domain of the amyloid precursor protein. *J. Biol. Chem. 286*, 39794−39803.
(98) Page, R. M., Gutsmiedl, A., Fukumori, A., Winkler, E., Haass, C., and Steiner, H. (2010) Beta-amyloid precursor protein mutants respond to gamma-secretase modulators. *J. Biol. Chem. 285*, 17798−17810.